Carnegie Observatories Astrophysics Series, Vol. 4:
Origin and Evolution of the Elements, 2004
ed. A. McWilliam and M. Rauch (Cambridge: Cambridge Univ. Press)

Chemical Evolution in ω Centauri

VERNE V. SMITH
Department of Physics, University of Texas at El Paso

Abstract

The globular cluster ω Centauri displays evidence of a complex star formation history and peculiar internal chemical evolution, setting it apart from essentially all other globular clusters of the Milky Way. In this review we discuss the nature of the chemical evolution that has occurred within ω Cen and attempt to construct a simple scenario to explain its chemistry. We conclude that its chemical evolutionary history can be understood as that which can occur in a small galaxy or stellar system ($M \approx 10^7 M_\odot$), undergoing discrete star formation episodes occurring over several Gyr, with substantial amounts of stellar ejecta lost from the system.

1.1 Introduction

Due to its distinctive chemical evolutionary history, the single globular cluster ω Cen certainly deserves mention in a meeting on the origin of the elements. Being the most massive known Galactic globular cluster, with a mass of $M \approx 3 \times 10^6 M_\odot$ (Merritt, Meylan, & Mayor 1997), it is almost as massive as a small dwarf spheroidal galaxy, such as Sculptor ($M \approx 6.5 \times 10^6 M_\odot$; Mateo 1998). Indeed, it has been argued that ω Cen is the surviving remnant of a larger system, such as a small galaxy, which was captured into a retrograde Galactic orbit in the distant past (Majewski et al. 2000; Gnedin et al. 2002). It should be mentioned that ω Cen was the topic of a recent meeting (in 2001), where all aspects of its nature were discussed; a large number of topics were covered, not just its chemical evolution, and this broader view of the cluster is well presented in the proceedings of that meeting (van Leeuwen, Hughes, & Piotto 2002).

ω Cen displays a number of fascinating traits that need to be noted in order to place it within the larger context of chemical evolution in various types of stellar systems or populations. First, ω Cen is the only known globular cluster to exhibit a large degree of chemical self-enrichment in all elements studied. Its iron abundance, for example, ranges from [Fe/H] $\approx$ –2.0, at the low end, up to $\sim$–0.40, where the bracket notation is defined as [A/B] = $\log(N_\mathrm{A}/N_\mathrm{B})_\mathrm{ProgramObject} - \log(N_\mathrm{A}/N_\mathrm{B})_\mathrm{Sun}$. The signature of this abundance spread was first detected as a large width in $(B-V)$ color of the giant branch in ω Cen from the photographic color-magnitude diagram of Woolley (1966). This giant branch "width" was confirmed photoelectrically by Cannon & Stobie (1973), who suggested that the color spread was due to varying metallicity. The inferred range in the heavy-element abundances (specifically the calcium abundance) was verified spectroscopically by Freeman & Rodgers (1975) using low-resolution spectra.

A second important trait of ω Cen is that the abundance distribution of the elements evolved in a most peculiar way as the metallicity (e.g., the Fe or Ca abundance) increased. As noted by Lloyd Evans (1977), the Ba II λ4554 Å line in ω Cen giants is considerably stronger than in 47 Tuc giants of similar luminosity and metallicity. In a following paper, Lloyd Evans (1983) identified a cool population of giants in ω Cen with strong ZrO bands, a characteristic of the *s*-process heavy-element-rich MS and S stars. Both Ba and Zr are produced in slow neutron capture (*s*-process) nucleosynthesis that occurs during shell He-burning thermal pulses in asymptotic giant branch (AGB) stars: recent extensive reviews covering the *s*-process and AGB evolution can be found in Wallerstein et al. (1997) and Busso, Gallino, & Wasserburg (1999). The ω Cen MS and S stars identified by Lloyd Evans are of lower luminosity than typical Galactic or Magellanic Cloud MS and S stars, which are AGB stars undergoing thermal pulses and the dredge-up of ^{12}C and *s*-process neutron capture elements. Since the giants found to be *s*-process rich in ω Cen are not luminous enough to be thermally pulsing AGB stars (and, thus, could not have self-enriched their own atmospheres with ^{12}C and *s*-process elements), Lloyd Evans (1983) argued that these chemically peculiar stars, which tend to be the more metal-rich stars, formed from gas that had been heavily enriched in *s*-process elements. Such an enrichment would presumably have been driven by extensive pollution from a previous population of AGB stars.

Subsequent high-resolution spectroscopic abundance studies of ω Cen giants by Francois, Spite, & Spite (1988), Paltoglou & Norris (1989), and Vanture, Wallerstein, & Brown (1994) found that the *s*-process elemental abundances (such as Y, Zr, Ba, or Nd) increase as the overall metallicity (i.e. [Fe/H]) increases; the *s*-process increase is enormous relative to other elements (such as Ca, Fe, or Ni). These detailed abundance studies confirm the Lloyd Evans hypothesis that there is a large *s*-process component involved in the overall chemical evolution within ω Cen.

A third trait that defines the character of ω Cen is that it is not only chemically peculiar, but also dynamically complex. Based on Ca abundances derived from low-resolution spectra, Norris, Freeman, & Mighell (1996) identified two distinct populations: a "metal-poor" component, with [Ca/H] ≈ -1.4 and containing about 80% of the stars, and a "metal-rich" one comprising the other 20%, with [Ca/H] ≈ -0.9. Later work by Norris et al. (1997), using radial velocities of the cluster members, revealed that the metal-poor and metal-rich populations were kinematically distinct. The metal-poor component is rotating (with $V_{\rm rot} \approx$ 5 km s^{-1}), while the metal-rich component is not. The metal-rich population is also more centrally condensed and has a lower velocity dispersion (or is kinematically cooler). Norris et al. (1997) interpreted these observations as being due to some type of merger in the proto-ω Cen environment.

More complexity was added to the two-population abundances and kinematics from Norris et al. (1996, 1997) by the discovery of increasingly metal-rich components (a third and a fourth) by Pancino et al. (2000), based on red giant branch (RGB) morphology. These additional metal-rich populations comprise about 5% of all ω Cen members. These newly discovered metal-rich stars became even more interesting when Ferraro, Bellazzini, & Pancino (2002) found them to display coherent, bulk motion with respect to the rest of the cluster stars. A subpopulation with its own distinct space motion would suggest a merger, and probably a recent one, as playing a role in the evolution of ω Cen to its present state.

This potentially fascinating result has been questioned by Platais et al. (2003), who point out that a color term has introduced systematic effects in the proper motions that could be responsible for the apparent bulk motion of the most metal-rich ω Cen members. This question remains open and no doubt will lead to new observations.

Recent accurate color-magnitude diagrams have also revealed details of the star formation history of ω Cen than can shed light on the nature of its chemical evolution. Hughes & Wallerstein (2000) used Strömgren photometry to derive an age-metallicity relation. They found that the metal-poor stars were typically 3 Gyr older than the metal-rich population, and then argue that this indicates that ω Cen enriched itself over this time scale. Hilker & Richtler (2000) also studied a large sample of ω Cen stars using Strömgren photometry and came to essentially the same conclusions as Hughes & Wallerstein (2000), although Hilker & Richtler suggest a slightly longer time scale of $\sim$6 Gyr for chemical enrichment. A very large color-magnitude diagram study (with 130,000 stars) by Lee et al. (2002) points to discrete, multiple stellar populations in ω Cen—not necessarily a continuous distribution of ages. Their modeling of the color-magnitude diagram suggests four distinct populations in ω Cen. This result may then agree quite nicely with the abundance distributions from Suntzeff & Kraft (1996), Norris et al. (1996), or Pancino et al. (2000). Although Norris et al. (1996) only identified two populations, while Suntzeff & Kraft (1996) pointed to a metal-rich tail, the two most metal-rich components in ω Cen only comprise a tiny fraction ($\sim$5%) of the total number of members.

We will now focus the remainder of this review on trying to understand the detailed nature of chemical evolution in ω Cen, within the framework of the metallicities, kinematics, ages, and star formation history as discussed above. A simple picture of its chemical evolutionary history will be sketched, with the predictions from this simple model compared to the observed abundances.

1.2 The Abundance Distribution and Chemical Enrichment

Both Suntzeff & Kraft (1996) and Norris et al. (1996) present relatively large samples of metallicities in ω Cen members derived from low-resolution spectra of the Ca II infrared (IR) triplet lines. Both studies endeavored to obtain unbiased samples of stars, with no selection criteria based on color or abundance. Norris et al. (1996) focused on giants brighter than $M_V = -1$ and presented a sample containing 521 stars. Suntzeff & Kraft (1996) studied two separate samples, one of subgiants with V magnitudes similar to those of the horizontal branch (199 members), as well as a sample of bright giants (144 members). In both studies, the Ca II equivalent widths were transformed onto metallicity scales by using calibrating globular clusters (47 Tuc, M4, NGC 6752 and NGC 6397 for Norris et al. and 47 Tuc, M71, M4, and NGC 6397 for Suntzeff & Kraft), with Suntzeff & Kraft (1996) tying their scale to the cluster [Fe/H] values, while Norris et al. (1996) opted to tie their scale to their own calibration in the clusters of [Ca/H].

The resulting metallicity distributions from Suntzeff & Kraft (1996) and Norris et al. (1996) are shown in Figure 1.1. Both studies find essentially the same distribution, but calibrated on different scales ([Fe/H] and [Ca/H]). There is a sharp cutoff in the number of stars toward low metallicities, with the sharpness set by the observational uncertainty. There is also a well-defined high-metallicity "tail" containing about 20% of the members. Suntzeff & Kraft (1996) tried fitting the metallicity distribution with a simple one-zone model of chemical evolution with instantaneous recycling. No satisfactory fit to the ω Cen metallicity

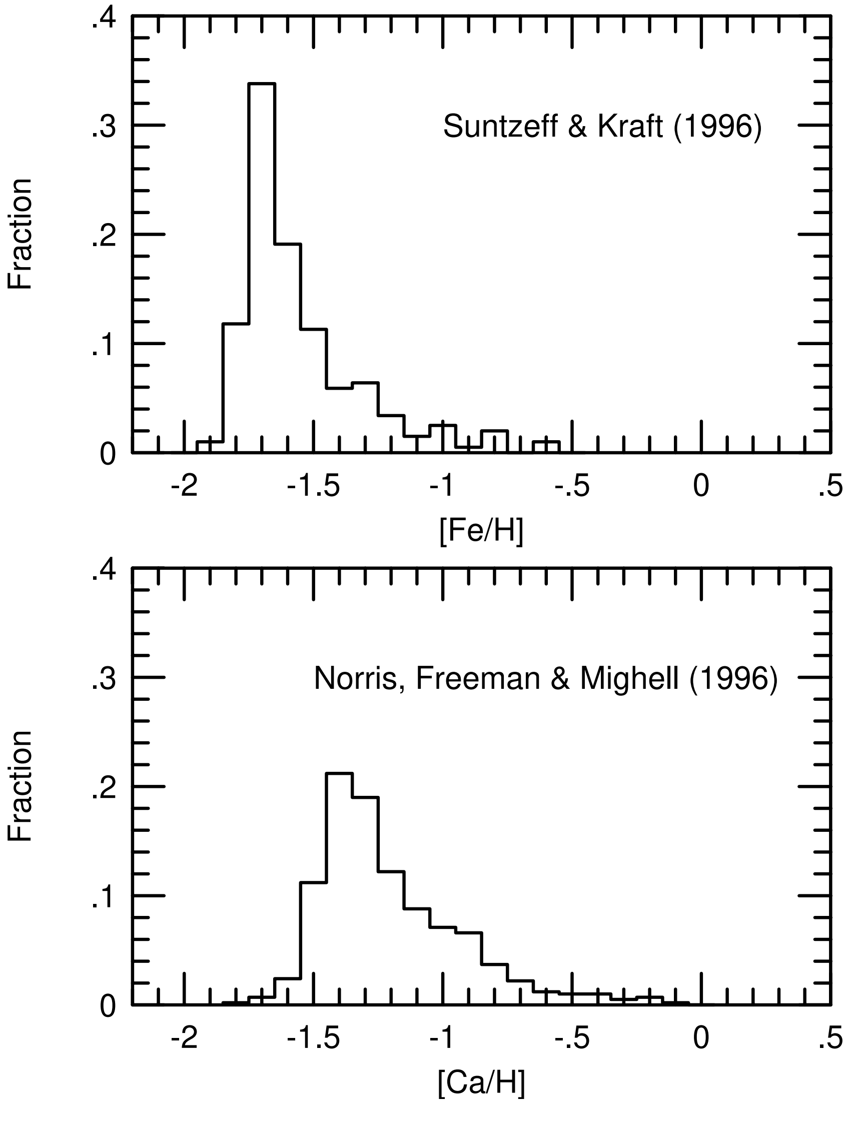

Fig. 1.1. Abundance distributions for samples of ω Cen members from Suntzeff & Kraft (1996) and Norris et al. (1996). The two "metallicity" distributions are tied to different scales, with [Fe/H] for Suntzeff & Kraft and [Ca/H] for Norris et al., but their shapes are very similar. Norris et al. (1996) fit two distinct populations to their distribution, which basically agrees with the metal-rich tail noted by Suntzeff & Kraft (1996).

distribution could be found from such a model; large effective yields from primary nucleosynthesis products are needed to fit the metal-rich tail, but such yields result in too broad of a peak in the metallicity distribution. Lower effective yields, which can fit the width of the main metallicity peak, fail to fit the metal-rich tail. Suntzeff & Kraft do point out that these two problems can be overcome if two generations of star formation are considered. Norris et al. (1996) consider slightly different types of models, where the cluster enrichment has occurred within a cloud of gas having some initial heavy-element enrichment, followed by further enrichment from stellar ejecta, with the total metallicity distribution being fit by two such components. Such a model can fit the [Ca/H] distribution, indicating two rather distinct populations in ω Cen. This population picture fits nicely into the later kinematic work from Norris et al. (1997), which finds two kinematic components that correlate with the metallicity, as discussed here in §1.1.

One possible consistent picture for the chemical evolution within ω Cen that fits the metallicity distributions discussed above would contain an initial population of stars with a very narrow range of metallicity: Suntzeff & Kraft (1996) estimate σ[Fe/H]$\leq$ 0.07 dex, based upon the sharpness of the low-metallicity cutoff. This narrow metallicity range is similar to what is found in other globular clusters, where typically σ[Fe/H]$\leq$ 0.05 dex (Suntzeff 1993). This initial generation of stars then pollutes the immediate interstellar medium (ISM) within the proto-ω Cen, and a second generation of stars is formed from this enriched material, with the new stars forming from different amounts of enriched material, giving rise to the broad high-metallicity tail. This simple picture does not address the cause of the second star formation episode, or whether such a scenario might be related to some sort of merger event, but it can, in very broad terms, account for the overall metallicity distribution. Additional support for a model using discrete star formation episodes comes from the more recent work on the RGB morphology from Pancino et al. (2000) and the color-magnitude diagram from Lee et al. (2002): both studies identify four distinct populations. As the most metal-rich third and fourth components account for only $\sim$5% of the members, just considering a two-epoch star formation model, as suggested by Suntzeff & Kraft (1996) and Norris et al. (1996), is probably adequate as a start. Such a model will be considered by us in §1.4; however, before applying this model, a more detailed discussion of the nature of the various types of elements involved in the chemical evolution within ω Cen is in order.

1.3 Abundance Ratios and the Nature of Chemical Evolution in ω Cen

Within a given stellar population, chemical evolution is driven by nucleosynthesis averaged over the stellar mass range and subsequent dispersal of this processed material back into the ISM. This heavy-element enrichment over time depends on such processes as star formation history, internal stellar evolution and nucleosynthesis as a function of mass, how stars return their processed ejecta back into the ISM, and whether some of the stellar ejecta can be lost from the system. By increasing the number of elements considered in an abundance analysis, we can obtain a more detailed picture of chemical evolution within ω Cen. In particular, elements that arise from different types of nucleosynthetic processes occurring in stars of differing masses provide more constraints on the chemical evolution.

In its simplest form, one might consider three basic stellar groups as contributing to most of a population's chemical evolution:

- High-mass stars ($M \geq 8-11 M_{\odot}$) that explode as supernovae of Type II (SNe II) and that contribute much of the heavy-element enrichment, such as O, Mg, Si, Ca, Ti, and some Fe, as well as the heavy neutron-rich, rapid neutron capture elements, personified, for example, by the element europium. Such stars can contribute their processed ejecta to a population's chemical enrichment on fairly short time scales ($\sim 10^7-10^8$ yr).

- Low- and intermediate-mass stars ($M \approx 1.0-8.0M_{\odot}$) that evolve onto the RGB and AGB and lose much of their mass via low-velocity stellar winds as red giants. Such winds contain material processed through the stellar interior that has been mixed to the surface via various red giant dredge-up episodes. The red giant winds from AGB stars might contribute significant yields of ^{12}C or ^{14}N, and substantial amounts of the heavy elements produced by the slow capture of neutrons, the *s*-process, as typified by such elements as Y, Zr, Ba, or La. These types of stars will contribute to chemical evolution over fairly long time scales of $\geq 10^8$–10^9 yr.
- Supernovae of Type Ia (SNe Ia), which almost certainly result from mass transfer in a binary driving a white dwarf over the Chandrasekhar mass limit. Such supernovae are expected to provide very large mass yields of Fe, and these systems can dominate Fe production in a stellar population over long time scales of $\sim$1 Gyr.

This is an admittedly thin sketch of stellar nucleosynthesis, but this is a limited review and the above points allow us to now investigate a few of the interesting points concerning chemical evolution within ω Cen in light of basic stellar nucleosynthesis.

The ability to detect and analyze a number of different elements, some of quite low abundance or represented by weak spectral lines, requires high-resolution spectra, with $R \equiv \lambda/\Delta\lambda \geq 18,000$, and preferably even higher, with $R = 35,000-60,000$. The results from high-resolution spectroscopic studies that are discussed here come from a number of studies that combine both high spectral resolution and high signal-to-noise ratio (S/N $\approx$ 50–100 or better). The largest such study to date is that of Norris & Da Costa (1995), who studied some 40 red giant members, but sacrificed a bit in S/N. Smaller samples, but with better S/N, include those of Francois et al. (1988), Smith, Cunha, & Lambert (1995), Smith et al. (2000), or Vanture, Wallerstein, & Suntzeff (2002). All of the studies mentioned above include a wide range of elements, while additional high-resolution analyses by Brown & Wallerstein (1993) or Pancino et al. (2002) contain elements produced by SNe II and SNe Ia, but do not include analyses of the *s*-process elements. Cunha et al. (2002) probe some 40 ω Cen giants, but focus on their copper abundances. All of these high-resolution results will be combined and discussed in the following two subsections, with the goal being to define the nature of the nucleosynthesis that is needed to explain the chemical enrichment observed in ω Cen.

1.3.1 The *s*-Process and AGB Stars

As first pointed out by Lloyd Evans (1983), the metal-enriched stars in ω Cen exhibit an overabundance of *s*-process elements. This increase is illustrated quantitatively in Figure 1.2, where we plot [Y/Fe] (top panel), [La/Fe] (middle panel), and [Eu/Fe] (bottom panel) versus A(Fe), where A(x) = log [N(x)/N(H)] + 12, from a number of different studies. We note that we have examined each abundance study to ascertain the sources of their respective gf-values and have put all of these different results on a common scale, when possible (we also adopt a solar Fe abundance of A(Fe) = 7.50). Yttrium and lanthanum are picked to represent the *s*-process, with Y (Z = 39) being a "light" *s*-process element and La (Z = 57) being a "heavy" *s*-process element. The abundance ratio of light to a heavy *s*-process elements is a diagnostic of the exposure to neutrons experienced by the material. Both elements are also spectroscopically well-observed species. Europium is included as a monitor of *r*-process nucleosynthesis. It is thought that most of the *s*-process abundances result from nucleosynthesis in AGB stars, while the *r*-process elements are synthesized in

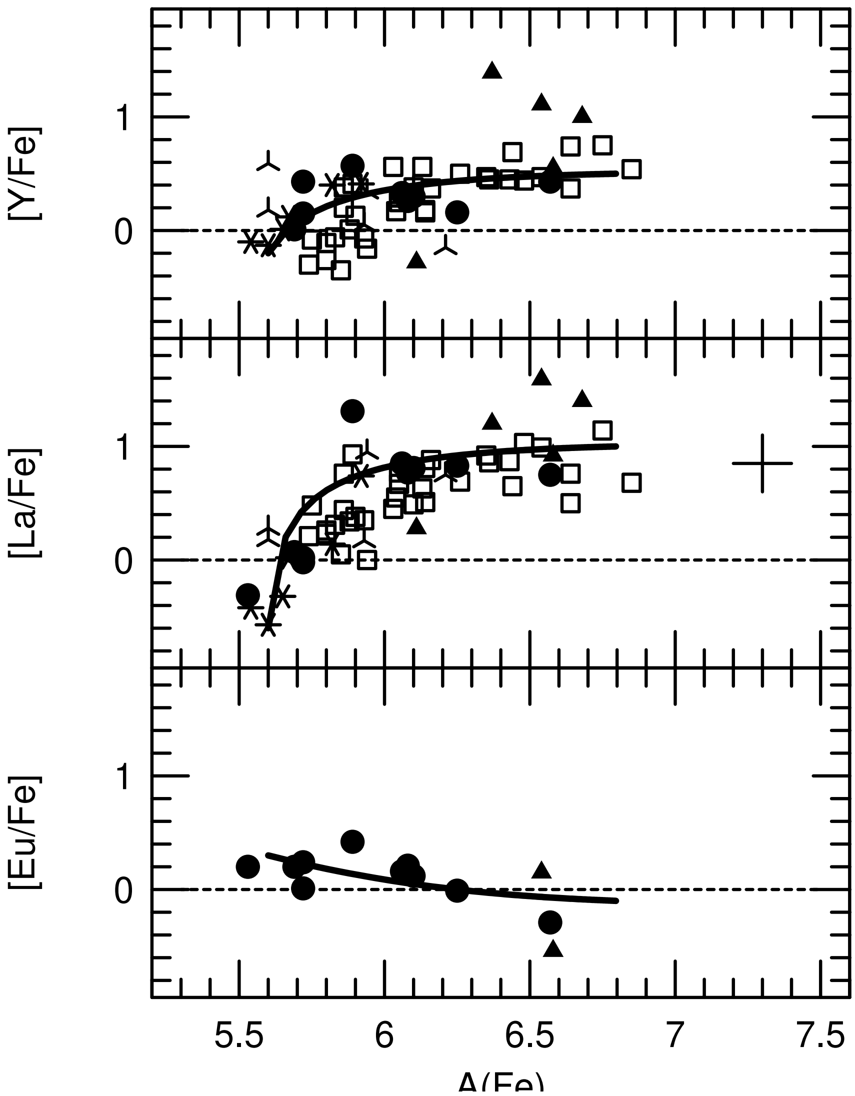

Fig. 1.2. Heavy-element abundance ratios in ω Cen showing light and heavy *s*-process elements Y and La, respectively, in the top and middle panels, along with the *r*-process element Eu in the bottom panel. The 6-pointed asterisks are from Francois et al. (1988), open squares from Norris & Da Costa (1995), 3-pointed symbols from Smith et al. (1995), filled circles from Smith et al. (2000), and filled triangles from Vanture et al. (2002). The set of error bars shown in the middle panel illustrates a typical internal uncertainty. As Fe increases by a factor of 10 in abundance, there is an enormous increase in [La/Fe] ($\sim$100 times), a large increase in [Y/Fe] ($\sim$10 times), and no increase (and perhaps a slight decrease) in [Eu/Fe]. This is a strong signature of *s*-process enrichment from low-metallicity, low-mass AGB stars. The solid curves in all three panels are what is expected from a chemical evolutionary scenario discussed in §1.4.

SNe II (for a review of these neutron capture processes and their relation to stellar evolution, see Wallerstein et al. 1997). Sample error bars are shown in the middle panel of Figure 1.2 to illustrate approximate internal abundance uncertainties in each study (adding error bars to each point would overwhelm the plotted points). All of the high-resolution studies highlighted in these discussions use similar quality spectra and similar analysis techniques. As the Fe abundance increases in ω Cen, the *s*-process component increases dramatically (Y and La), with no such increase in the *r*-process (Eu). The enormous [*s*-process/Fe] abundance ratios found in the general population of the more metal-rich ω Cen stars have not been found in general stellar populations associated with the Milky Way halo or disk. Recent abundances derived in red giants of the Sagitarrius dwarf galaxy by Smecker-Hane & McWilliam (2004), however, do show large *s*-process to iron ratios as observed in ω Cen. The solid curves in Figure 1.2 are predictions from a simple two-component star formation plus mixing scheme of chemical evolution that is discussed in §1.4.

A key point of Figure 1.2 is that the increase in [La/Fe] is larger than the increase in [Y/Fe], meaning that the overall ratio of La/Y in the *s*-process material that has enriched ω Cen has a value of [La/Y] $\approx$ +0.4 to +0.5. This excess of La over Y is a signature of low-mass, low-metallicity AGB stars driving the *s*-process; Busso et al. (1999) provide a detailed review of the various types of *s*-process abundance distributions expected from AGB stars of various masses and metallicities.

Smith et al. (2000) compared the heavy-element abundances in ω Cen with predictions from models of AGB nucleosynthesis at the appropriate metallicities and found that 1.5 $M_\odot$ models yield the best overall fits to the *s*-process abundance distributions in the *s*-process-enriched members. The heavy-element abundances in the ω Cen stars thus point to low-mass AGB stars as dominating the *s*-process enrichment in this cluster. The lifetimes of these lower-mass stars are of order 3 Gyr, pointing to a protracted period of star formation, evolution, and chemical enrichment in ω Cen. This time scale agrees with the results from Hughes & Wallerstein (2000) and Hilker & Richtler (2000), who find age spreads of 3–6 Gyr based upon Strömgren photometry and main sequence isochrones (for Hughes & Wallerstein), and red giant isochrones (for Hilker & Richtler).

1.3.2 The α-Elements and Contributions from Supernovae

As reviewed by McWilliam (1997), it has been shown observationally by many investigations over many years that even-Z elements, such as O, Mg, Si, S, Ca, and Ti, are overabundant relative to Fe in almost all Galactic metal-poor stars. This mix of elements is often referred to collectively as the α-elements, although this collectivization should not be taken to imply that these elements are all produced in uniform ratios in a single type of object. All of the α-elements are produced in SNe II (e.g., Woosley & Weaver 1995), but their respective yields depend on such variables as stellar mass or metallicity. The general trend found in the majority of metal-poor Galactic disk and halo stars is that, for iron abundances of [Fe/H]$\leq$ –1.0, the values of [α/Fe] $\approx$ +0.2 to +0.6 and are roughly constant with metallicity, but having different values of [α/Fe] for the different elements. At iron abundances [Fe/H]$\geq$–1.0, there is a quasi-linear decrease in [α/Fe] toward 0.0 as [Fe/H] approaches 0.0. The behavior of [α/Fe] versus [Fe/H] is usually interpreted to result from the time delay between SN II contributions to chemical evolution relative to the contributions from SNe Ia. The beginning of the decrease in the values of [α/Fe] is then due to the onset of SNe Ia, which begin to add large amounts of Fe into a population's pool of heavy elements.

Abundances from three elements of the "α family" (Si, Ca, and Ti) in ω Cen are shown in Figure 1.3, plotted as [x/Fe] versus A(Fe). The top panel shows [Si/Fe], the middle [Ca/Fe], and the bottom [Ti/Fe] taken from a number of studies noted in the figure caption. Missing from this figure are [O/Fe] and [Mg/Fe] because, as discussed in both Norris & Da Costa (1995) and Smith et al. (2000), ω Cen red giants show large ranges in, and anti-correlated behavior between, [O/Fe] and [Na/Fe], which is often seen in other globular clusters but not in the field red giants; for a review of this effect, see Kraft (1994). This abundance pattern reveals the effects of H-burning by both the ON part of the CNO cycles, as well as the Ne-Na cycle. It is still not clear to what extent these O and Na (as well as Al and Mg) abundance variations observed in the globular cluster-like populations may be due to red giant mixing within the giant itself, or patterns that were imprinted on the currently observed stars by a previous stellar generation. Whatever the fundamental cause, oxygen, sodium, aluminum, and magnesium abundances in ω Cen may have been altered by nuclear processes that have nothing to do with SNe II; thus, O and Mg are omitted from Figure 1.3.

In the middle panel are shown horizontal bars that schematically represent the approximate metallicities [in A(Fe)] of ω Cen subpopulations as identified by Pancino et al. (2000). The most metal-poor component is labeled RGB-MP, with RGB-Int being the intermediate-metallicity group and the extremely metal-rich population (identified by Pancino et al.) is RGB-a. Recall that RGB-MP and RGB-Int correspond to the metal-poor and metal-rich ω Cen stars identified by Norris et al. (1996) and Suntzeff & Kraft (1996), with these two subpopulations accounting for about 95% of the ω Cen members. In the metallicity range corresponding to RGB-MP and RGB-Int, the α-element to iron abundance ratios look indistinguishable from those of Galactic halo stars. Over the range of iron abundances of A(Fe) = 5.5 to 6.5 there are no strong trends of [Si/Fe], [Ca/Fe], or [Ti/Fe], and the respective values of [X/Fe] for these elements in ω Cen are essentially the same as found for the majority of Galactic metal-poor field halo stars between the same metallicity limits. There may be slight increases in the values of each of these [α/Fe] ratios as A(Fe) increases (with slopes of $\sim$+0.1 to +0.2 dex per dex), although the significance of these possible trends needs to be assessed with a larger, homogeneous analysis. The positive values of [α/Fe] in the ω Cen subpopulations RGB-MP and RGB-Int indicate chemical evolution in an environment in which SNe II control the nucleosynthesis (with little, or no significant, contribution from SNe Ia).

The situation for the RGB-a subpopulation may be different, as there are indications from the results of Pancino et al. (2002), as shown in Figure 1.3, that [Si/Fe] and [Ca/Fe] may decrease relative to the values for RGB-MP and RGB-Int. This may indicate that the RGB-a members are showing measurable amounts of Fe produced from SNe Ia. If so, this is probably not due to a simple time scale difference between chemical evolution in RGB-MP and RGB-Int compared to RGB-a. Recall from §1.3.1 that the substantial build-up in the *s*-process abundances from RGB-MP to RGB-Int requires time scales of $\sim$1–3 Gyr. This time scale estimate based on low-mass stellar evolution to the AGB is also in agreement with the color-magnitude main sequence turn-off results from Hughes & Wallerstein (2000) and Hilker & Richtler (2000). Such times are longer than expected for SNe Ia to affect chemical evolution. In their study of copper abundance in 40 ω Cen members, Cunha et al. (2002) discuss this time scale discrepancy between AGB and SN Ia chemical enrichment and speculate on two possible reasons. One suggestion is that the stellar density in ω Cen was so large that binary systems that would lead eventually to SNe Ia were disrupted. Another

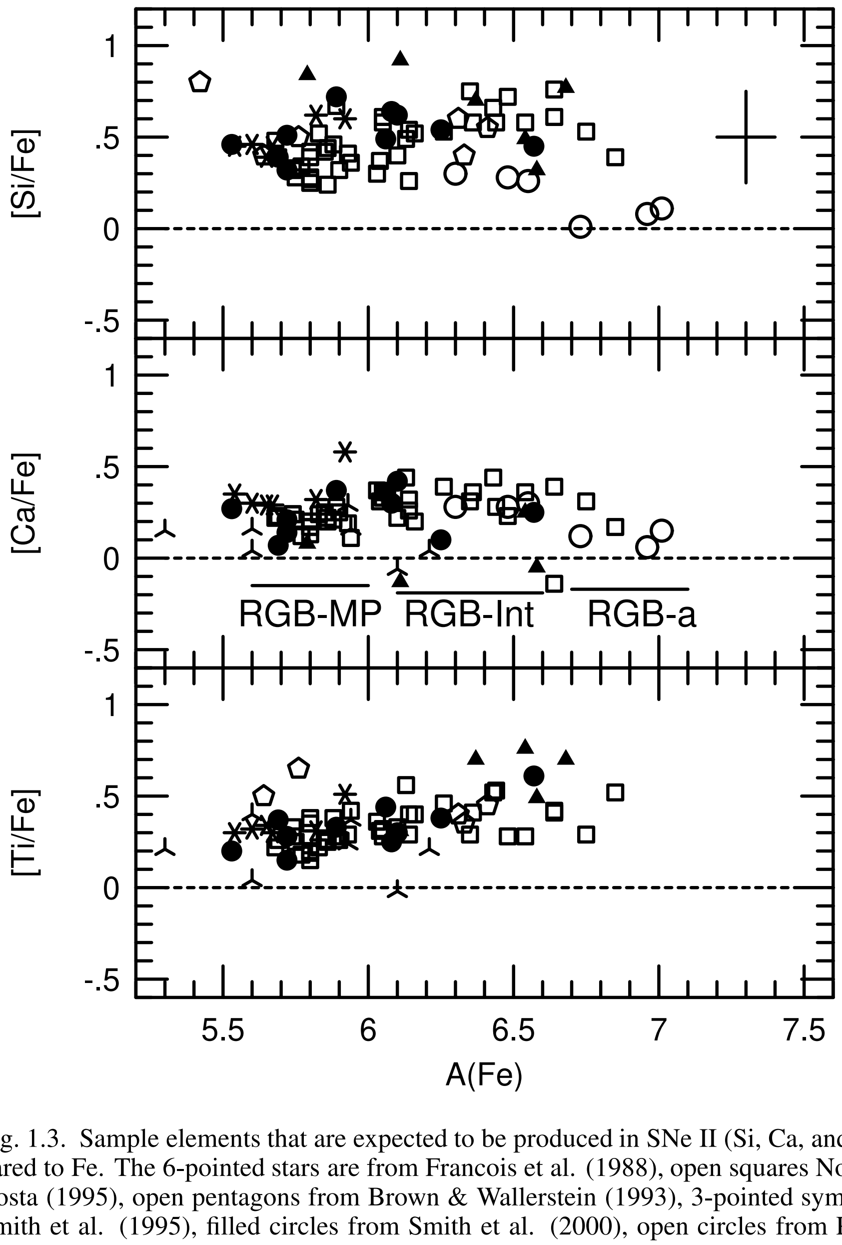

Fig. 1.3. Sample elements that are expected to be produced in SNe II (Si, Ca, and Ti) compared to Fe. The 6-pointed stars are from Francois et al. (1988), open squares Norris & Da Costa (1995), open pentagons from Brown & Wallerstein (1993), 3-pointed symbols from Smith et al. (1995), filled circles from Smith et al. (2000), open circles from Pancino et al. (2002), and filled triangles from Vanture et al. (2002). A typical internal uncertainty is shown by the error bars in the top panel. In the middle panel, the horizontal lines represent the approximate Fe abundances of the subpopulations identified by Pancino et al. (2000): RGB-MP (for metal-poor red giants), RGB-Int (for the intermediate-metallicity giants), and RGB-a (for the more metal-rich subpopulation). In the RGB-MP and RGB-Int red giants, all three of the α-elements shown are overabundant relative to Fe, as found in most Galactic halo stars. The RGB-a members may show hints of decreasing values in [Si/Fe] and [Ca/Fe], suggestive of nucleosynthesis from SNe Ia.

possibility is that SN Ia ejecta have larger kinetic energies than SN II ejecta, leading to lower rates of effective enrichment from SNe Ia compared to SNe II. In order to solve this puzzle, a larger and more homogeneous analysis should be conducted to compare, in detail, the abundance distributions that characterize the various subpopulations in ω Cen—especially a study concentrating on the RGB-a members.

1.4 A Simple Model for the Chemical Evolution of ω Cen

1.4.1 α-Element and s-Process Abundances and Selective Retention of Stellar Ejecta

The increase in the overall Fe abundance in ω Cen, coupled to the enhanced ratios of [Si/Fe], [Ca/Fe], or [Ti/Fe]m points to chemical enrichment from SNe II. The possible decrease in both [Si/Fe] and [Ca/Fe] in the most metal-rich subpopulations of ω Cen suggests the eventual appearance of nucleosynthesis products from SNe Ia. In the context of SN enrichment, one puzzle in ω Cen is how to understand the large s-process (or AGB) component in its chemical enrichment. An initial mass function (IMF) deficient in high-mass stars is certainly one possibility. Another hypothesis, perhaps less extreme than altering the IMF, was explored by Smith et al. (2000) and Cunha et al. (2002). This hypothesis is that in the lowest-mass systems that undergo self-enrichment or internal chemical evolution, stellar ejecta or winds are retained preferentially within the system, or lost to the system, depending on their ejection velocities. In this picture, the high-velocity enriched ejecta from either SNe II or SNe Ia are retained inefficiently within the gravitational potential well of the system when compared to low-velocity AGB winds (heavily enriched in the s-process elements). Smith et al. (2000) modeled this chemical evolution numerically for a system with an initial mass of $10^7 M_\odot$ in which stars formed with the standard Salpeter IMF. The constraint on mass-ejecta retention required to fit the ω Cen abundances was that 10% of SN II ejecta, along with less than 10% of SN Ia ejecta (with SNe Ia becoming active after a time of 1.2 Gyr), were retained for future incorporation into new stars. The s-process-rich AGB ejecta were retained completely, however. In this simple model, the yields for the α-elements were taken from Woosley & Weaver (1995) and convolved with a Salpeter mass function to determine the chemical compositions of the SN II ejecta. Yields for the s-process were taken from the AGB models discussed in Smith et al. (2000). This straightforward exercise reproduces the general trends of SNe (e.g., Si or Ti) and AGB abundances in ω Cen, with the only novel assumption being that SN ejecta are much less efficiently retained than AGB ejecta.

1.4.2 Metallicity-dependent SN II Yields and the Star Formation History

Additional constraints on the nature of chemical evolution in ω Cen are provided by elements that show, or are predicted to have, metallicity-dependent SN II yields, such that [element/Fe] values will depend upon the metallicity of the parent SNe. Cunha et al. (2002) studied copper in 40 ω Cen giants and compared their results to those for field stars in the Galactic disk and halo from Sneden, Gratton, & Crocker (1991) and Mishenina et al. (2002). In the Galactic field stars, [Cu/Fe] shows a steady increase with increasing [Fe/H] over the range of –2.8 to –1.2 in [Fe/H], with a slope of $\sim$+0.12 dex per dex in [Cu/Fe] versus [Fe/H]. Sneden et al. (1991) attribute this general increase in [Cu/Fe] at low [Fe/H] as due to metallicity-dependent yields for Cu from SNe II. Within the interval of –1.2 to –1.0 in [Fe/H], [Cu/Fe] increases rapidly from –0.5 to +0.0, and then stays at this value up to a solar iron abundance. This steep increase in [Cu/Fe] is probably due to Cu production from SNe Ia. In contrast to the Galactic field, Cunha et al. (2002) find that [Cu/Fe] is constant in ω Cen, at ∼–0.55, from [Fe/H] = –2.0 up to –0.80. At the higher iron abundances, where [Fe/H] = –1.0 to –0.8, the ω Cen stars are falling significantly below the Galactic field trend (by ∼–0.5 dex in [Cu/Fe] at [Fe/H] = –0.8). Pancino et al. (2002) also derived [Cu/Fe] in six ω Cen stars over the range of –1.2 to –0.4 in [Fe/H]. Their copper abundance values overlap those of Cunha et al. (2002) nicely and confirm the low values of [Cu/Fe] in ω Cen. The most metal-rich giant in the Pancino et al. sample is trending upwards in [Cu/Fe] and may signal the measurable addition of SN Ia ejecta, as suggested for some of their results for [Si/Fe] and [Ca/Fe]. Recently, Simmerer et al. (2003) have sampled [Cu/Fe] in 10 "mono-metallicity" globular clusters and find that its behavior with [Fe/H] in these more typical globular clusters is indistinguishable from the Galactic field. Simmerer et al. (2003) conclude that the slow increase in [Cu/Fe] with [Fe/H] at low metallicities results from metallicity-dependent yields from SNe II (as indicated by earlier studies; e.g, Sneden et al. 1991). In addition, they suggest that the rapid increase from [Cu/Fe] ≈ –0.5 to +0.0 between [Fe/H] = –1.2 to –1.0 is probably due to the substantial input of Cu from SNe Ia (as argued by Matteucci et al. 1993).

Adding to the interesting differences in [Cu/Fe] between ω Cen and the Galactic field stars are the first abundances obtained for fluorine by Cunha et al. (2003). These initial results provide tantalizing hints that fluorine behaves similarly to copper in a comparison of ω Cen stars with field-star samples from the Galaxy and the Large Magellanic Cloud (LMC). In the case of fluorine, Cunha et al. (2003) found that a sample of five ω Cen giants displayed values of [F/O] that were significantly lower than the [F/O] ratios found in in Galactic and LMC field red giants having the same oxygen abundances. They also found that the trend in [F/O] versus A(O) defined by the Galactic and LMC stars agreed reasonably well with the predictions of chemical evolutionary models from Timmes, Woosley, & Weaver (1995) and Alibes, Labay, & Canal (2001), in which fluorine production is driven primarily by neutrino spallation off of ^{20}Ne during SN core collapse, as described by Woosley et al. (1990). These models predict a metallicity-dependent decline in [F/O] versus A(O) of about –0.30 dex per dex.

Cunha et al. (2003) suggested a scenario to explain the behavior of [F/O] in ω Cen (as well as [Cu/Fe]), in comparison to the field-star behaviors in the Galaxy and the LMC (for fluorine), by considering the possible star formation history of ω Cen. Their working assumption is that ω Cen underwent a few (2–4) well-separated star formation episodes many Gyr ago: this assumption is motivated by the morphology of the color-magnitude diagram (e.g., Lee et al. 2002). In the simplest case of two star formation episodes (that seem to account for ∼95% of the members, as found in the [Ca/H] distribution from Norris et al. 1996), some fraction of ejecta from the first stellar generation is retained with the ω Cen proto-system (with only a small fraction of SNe II retained, even less from SNe Ia, but 100% of AGB ejecta). This retained ejecta is then mixed with a reservoir of very metal-poor gas; this reservoir may represent the infall, or merging, of a primordial (or less chemically evolved) cloud that might itself induce the second episode of star formation. If the newly added metal-poor gas and the ejecta gas are mixed inhomogeneously, stars of the second generation will have a spread of heavy-element abundances, as observed in ω Cen. Abundance ratios, on the other hand, will be nearly constant in all stars as long as the infalling (or merging) gas cloud is severely underabundant in those elements comprising a given ratio.

If an abundance ratio from SNe II is metallicity dependent, such as [Cu/Fe] or [F/O], then this ratio will appear anomalous (and will be $\sim$ constant with respect to [Fe/H] or [O/H]) when compared to stellar populations that form from gas that has undergone many star formation episodes in which stellar ejecta become well mixed with the ISM. In a sense, the abundance ratios carry the "memory" of the metallicities of the SNe II that formed the bulk of the ejecta out of which they formed. A comparison using abundance ratios insensitive to SN II metallicity (such as [Si/Fe] or [Ca/Fe]) will appear normal, as is observed in ω Cen.

1.4.3 Putting Together the Pieces of the Abundance Puzzle

The basic picture of an initial population of stars in the proto-ω Cen environment evolving and depositing ejecta, followed by a second stellar generation forming from a mixture of this ejecta and added metal-poor gas, can be tested for consistency by examining abundance ratios. In this scenario, the more metal-rich members are stars that formed from larger fractions of ejecta from the first population. The limiting case would be a star that formed from pure first generation ejecta. Thus, an approximate abundance distribution for the ejecta (or lower-limit elemental abundances to this gas) can be taken to be the abundances defined by the most metal-rich members of the second stellar generation. The additional metal-poor gas added to this mixture is taken to have much lower heavy-element abundances than the ejecta. The exact composition of this added gas is unknown, but limits to its metallicity can be deduced from the sharp low-metallicity cut-offs in the distributions derived by both Suntzeff & Kraft (1996) and Norris et al. (1996); see Figure 1.1. Both studies found that the sharpness (in either [Fe/H] or [Ca/H]) of this cut-off is set by their respective observational uncertainties: in principle, the low-metallicity cut-off could be a step function. This sharp boundary in the metallicity distribution at low values indicates that the gas in the proto-ω Cen system was "pre-enriched" and well mixed, as discussed in the chemical models employed by Norris et al. (1996). It is thus reasonable to use, as the composition of the added metal-poor gas that is incorporated into the second generation, this pre-enriched material that was already part of the proto-ω Cen system. In this case, stars that formed from differing amounts of these two reservoirs of material should follow a "mixing line" going from the most metal-poor to the most metal-rich stars. Referring back to Figure 1.2, where the heavy-element ratios of [Y/Fe], [La/Fe], and [Eu/Fe] are shown, the solid curves show such mixing lines, with the initial abundances taken as those defined by the metal-poor population. As discussed in Smith et al. (2000), the heavy-element abundance distribution in the most metal-poor ω Cen stars is characterized by an *r*-process distribution, but these abundances are then transformed into an *s*-process distribution as [Fe/H] increases. The *s*-process distribution, with [La/Y] $\approx$ +0.5 and [La/Eu] $\approx$ 1.2, is indicative of nucleosynthesis from low-mass, low-metallicity AGB stars, as reviewed by Busso et al. (1999). The mixing lines shown in Figure 1.2 are fair representations of the observed abundances of Y, La, and Eu.

Further consistency checks can be conducted using other abundance ratios. The transition from an *r*-process-dominated heavy-element distribution in the metal-poor, first stellar generation to a second generation with a strong *s*-process component should appear as a changing [La/Y] ratio (the [La/Eu] or [Y/Eu] ratios would be better, but most of the (few) Eu abundances derived in ω Cen stars are from the relatively small sample from Smith et al. 2000). The top panel of Figure 1.4 illustrates [La/Y] versus A(Fe) from a number of studies of ω Cen: note the very rapid rise in [La/Y] as a function of the iron abundance.

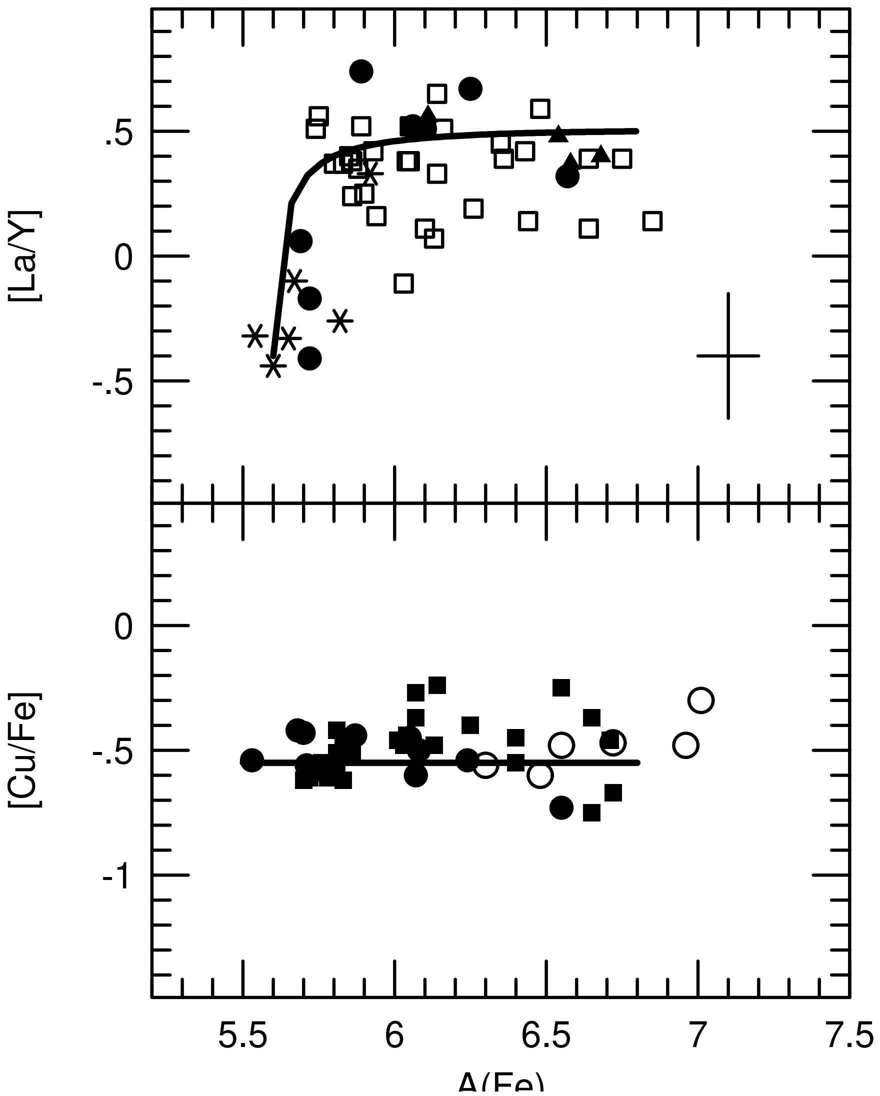

Fig. 1.4. The behavior of the heavy-element ratio of [La/Y] versus the iron abundance (top panel) and that of [Cu/Fe] (bottom panel). In the top panel, the 6-pointed stars are from Francois et al. (1988), open squares from Norris & Da Costa (1995), filled circles from Smith et al. (2000), and filled triangles from Vanture et al. (2002). In the bottom panel, the filled squares are from Cunha et al. (2002) and open circles from Pancino et al. (2002). A typical set of error bars are shown in the top panel. The increase in [La/Y] as A(Fe) increases is very steep (in the top panel), illustrating a transition from a heavy-element distribution dominated by the *r*-process to one dominated by the *s*-process. The solid curve is defined by the chemical evolutionary picture discussed in the text, and this curve tracks the behavior of the La/Y ratio well. The [Cu/Fe] values in ω Cen (bottom panel) show no measurable change as A(Fe) increases, unlike Galactic halo stars, which show increasing values of [Cu/Fe] over this metallicity range. If copper in these metal-poor populations is dominated by metallicity-dependent SN II yields, then the horizontal line is what is expected from the simple model of chemical evolution invoked here to understand ω Cen. In terms of the copper to iron abundance ratios, this model explains the observations.

The solid curve is the mixing line as set by the same curves used in Figure 1.2. Again, the simple two-component mixing model for chemical evolution in ω Cen provides an adequate description of the observed abundances.

The bottom panel of Figure 1.4 shows the results for [Cu/Fe] in ω Cen from Cunha et al. (2002) and Pancino et al. (2002). In Galactic field halo stars (Sneden et al. 1991; Mishenina et al. 2002) and other globular cluster stars (Simmerer et al. 2003), values of [Cu/Fe] increase steadily as A(Fe) increases from $\sim$4.7 to 6.5; this increase is interpreted as being due to metallicity-dependent SN II yields (e.g., Simmerer et al. 2003). No such increase is observed in ω Cen, and in the picture of a single-metallicity initial stellar population producing the SN II products from which a second generation of stars are born, a constant Cu/Fe ratio would be predicted, with the value of this ratio set by the metallicity of the first generation of SNe II. Such a constant copper to iron ratio is illustrated by the straight line in Figure 1.4, and this horizontal line is clearly a very good fit to the behavior of copper with iron. In addition, the value of [Cu/Fe] $\approx$ –0.55 is the value found in field halo stars with A(Fe) $\approx$ 5.5 (see Mishenina et al. 2002), which corresponds to the lowest metallicity ω Cen stars.

1.4.4 An Overview of Chemical Evolution and Star Formation in ω Cen

In summary, we advocate a picture of chemical evolution in ω Cen that is driven by a small number of distinct, time-separated star formation events; this picture is motivated by the color-magnitude morphology from, for example, Hughes & Wallerstein (2000), Hilker & Richtler (2000), or Lee et al. (2002). The large *s*-process abundance component, relative to elements produced in either SNe II or SNe Ia, in ω Cen's chemical enrichment points to AGB stars as playing a major role in chemical evolution (relative to the Galaxy). This could result from a different IMF, although we prefer to suggest that selective retention of stellar ejecta is the cause, with SN ejecta being retained less efficiently than AGB winds. Continuing star formation in ω Cen then results from the mixing of this stellar ejecta with additional gas arriving from outside of the spatial regions defined by the stars. We have taken this gas to be metal-poor, relative to the stellar ejecta, and find that the observed abundance trends can be fit by such a picture (the solid curves in Figures 1.2 and 1.4). We have focused on describing the first two generations in ω Cen for two reasons: (1) these first two stellar generations seem to account for 95% of the ω Cen members (Suntzeff & Kraft 1996; Norris et al. 1996; Pancino et al. 2000), and (2) the most metal-rich stars have yet to be analyzed in detail in terms of their abundance distributions.

The chemical evolution discussed above is similar to a picture suggested by Freeman (2002). In this scenario, ω Cen is the surviving nucleus of a small galaxy, with its abundance spread being established by the infall of enriched stellar ejecta from the surrounding galaxy into the nucleus. This is a variation from the picture presented above in the sense that enriched material is not retained within the spatial extent of the stars, but arrives from outside. The Freeman (2002) scenario may explain more easily the observed kinematic and angular momentum properties of ω Cen's subpopulations. Certainly larger samples of stars and more detailed abundance and kinematic studies will shed light on the details of the history of ω Cen.

1.5 Conclusions

ω Cen represents a fascinating and valuable object to those interested in studying chemical evolution across a variety of environments and populations. Although classified as a globular cluster, its complex star formation and chemical enrichment histories, plus retrograde Galactic orbit, place it in a different category than the more typical "mono-metallicity" globular clusters. It is almost certainly the remnant of a captured small galaxy that experienced, before its capture, a chemical enrichment history unlike that of any other known Galactic disk or halo population. Because ω Cen is relatively nearby, compared to other small galaxies of the Local Group, it can be used as a comparison template and laboratory in which to probe different aspects of chemical evolution that may occur in some small galaxies.

Acknowledgements. VVS acknowledges support for chemical abundance work from the National Science Foundation (AST99–87374) and NASA (NAG5–9213).

References

Alibes, A., Labay, J., & Canal, R. 2001, A&A, 370, 1103
Brown, J. A., & Wallerstein, G. 1993, AJ, 106, 133
Busso, M., Gallino, R., & Wasserburg, G. J. 1999, ARA&A, 37, 239
Cannon, R. D., & Stobie, R. S. 1973, MNRAS, 162, 207
Cunha, K., Smith, V. V., Lambert, D. L., & Hinkle, K. H. 2003, AJ, 126, 1305
Cunha, K., Smith, V. V., Suntzeff, N. B., Norris, J. E., Da Costa, G. S., & Plez, B. 2002, AJ, 124, 379
Ferraro, F. R., Bellazzini, M., & Pancino, E. 2002, ApJ, 573, L95
Francois, P., Spite, M., & Spite, F. 1988, A&A, 191, 267
Freeman, K. C. 2002, in ω Centauri: A Unique Window into Astrophysics, ed. F. van Leeuwen, J. D. Hughes, & G. Piotto (San Francisco: ASP), 423
Freeman, K. C., & Rodgers, A. W. 1975, ApJ, 201, L71
Gnedin, O. Y., Zhao, G., Pringle, J. E., Fall, S. M., Livio, M., & Meylan, G. 2002, ApJ, 568, L23
Hilker, M., & Richtler, T. 2000, A&A, 362, 895
Hughes, J. D., & Wallerstein, G. 2000, AJ, 119, 1225
Kraft, R. P. 1994, PASP, 106, 553
Lee, Y.-W., Rey, S.-C., Ree, C. H., & Joo, J.-M. 2002, in ω Centauri: A Unique Window into Astrophysics, ed. F. van Leeuwen, J. D. Hughes, & G. Piotto (San Francisco: ASP), 305
Lloyd Evans, T. 1977, MNRAS, 181, 591
——. 1983, MNRAS, 204, 975
Majewski, S. R., Patterson, R. J., Dinescu, D. I., Johnson, W. Y., Ostheimer, J. C., Kunkel, W. E., & Palma, C. 2000, in The Galactic Halo: From Globular Cluster to Field Stars, ed. A. Noels et al. (Liége: Institut d'Astrophysique et de Geophysique), 619
Mateo, M. L. 1998, ARA&A, 36, 435
Matteucci, F., Raiteri, C. M., Busso, M., Gallino, R., & Gratton, R. 1993, A&A, 272, 421
McWilliam, A. 1997, ARA&A, 35, 503
Merritt, D., Meylan, G., & Mayor, M. 1997, AJ, 114, 1074
Mishenina, T. V., Kovtyukh, V. V., Soubiran, C., Travaglio, C., & Busso, M. 2002, A&A, 396, 189
Norris, J. E., & Da Costa, G. S. 1995, ApJ, 447, 680
Norris, J. E., Freeman, K. C., Mayor, M., & Seitzer, P. 1997, ApJ, 487, L187
Norris, J. E., Freeman, K. C., & Mighell, K. J. 1996, ApJ, 462, 241
Paltoglou, G., & Norris, J. E. 1989, ApJ, 336, 185
Pancino, E., Ferraro, F. R., Bellazzini, M., Piotto, G., & Zoccali, M. 2000, ApJ, 534, L83
Pancino, E., Pasquini, L., Hill, V., Ferraro, F. R., & Bellazzini, M. 2002, ApJ, 568, L101
Platais, I., Wyse, R. F. G., Hebb, L., Lee, Y.-W., & Rey, S.-C. 2003, ApJ, 591, L127
Simmerer, J., Sneden, C., Ivans, I. I., Kraft, R. P., Shetrone, M. D., & Smith, V. V. 2003, AJ, 125, 2018
Smecker-Hane, T. A., & McWilliam, A. 2004, ApJ, submitted
Smith, V. V., Cunha, K., & Lambert, D. L. 1995, AJ, 110, 2827

Smith, V. V., Suntzeff, N. B., Cunha, K., Gallino, R., Busso, M., Lambert, D. L., & Straniero, O. 2000, AJ, 119, 1239

Sneden, C., Gratton, R., & Crocker, D. A. 1991, A&A, 246, 354

Suntzeff, N. B. 1993, in The Globular Cluster-Galaxy Connection, ed. G. H. Smith & J. P. Brodie (San Francisco: ASP), 167

Suntzeff, N. B., & Kraft, R. P. 1996, AJ, 111, 1913

Timmes, F. X., Woosley, S. E., & Weaver, T. A. 1995, ApJS, 98, 617

van Leeuwen, F., Hughes, J. D., & Piotto, G., ed. 2002, ω Centauri: A Unique Window into Astrophysics (San Francisco: ASP)

Vanture, A. D., Wallerstein, G., & Brown, J. A. 1994, PASP, 106, 835

Vanture, A. D., Wallerstein, G., & Suntzeff, N. B. 2002, ApJ, 564, 395

Wallerstein, G., et al. 1997, Rev. Mod. Phys., 69, 995

Woolley, R. R. 1966, Royal Observatory Annals No. 2

Woosley, S. E., Hartmann, D. H., Hoffman, R. D., & Haxton, W. C. 1990, ApJ, 356, 272

Woosley, S. E., & Weaver, T. A. 1995, ApJS, 101, 181